



Vanillin mediated green synthesis and application of gold nanoparticles for reversal of antimicrobial resistance in *Pseudomonas aeruginosa* clinical isolates



Sagar S. Arya^{a,b}, Mansi M. Sharma^c, Ratul K. Das^a, James Rookes^b, David Cahill^b, Sangram K. Lenka^{a,*}

^a TERI-Deakin Nanobiotechnology Centre, Gurgaon, Haryana, 122001, India

^b Deakin University, School of Life and Environmental Sciences, Waurn Ponds Campus, Geelong, Victoria, 3216, Australia

^c Center for Innovation Research and Consultancy, Pune, 411018, India

ARTICLE INFO

Keywords:

Microbiology
Nanotechnology
Materials science
Vanillin capped gold nanoparticles (VAuNPs)
Vanillin
Pseudomonas aeruginosa
Extreme drug resistance (XDR)
Antibiotic potentiation
MexAB-OprM efflux pump

ABSTRACT

Antimicrobial resistance (AMR) is a serious concern in pathogenic bacteria. As a new approach to addressing AMR, we report here the green synthesis of vanillin capped gold nanoparticles (VAuNPs) using the popular flavouring molecule vanillin (C₈H₈O₃) as a reducing and capping agent. Physicochemical characterization revealed that the synthesised VAuNPs were stable and crystalline in nature. VAuNPs were non-bactericidal even at high concentration (>2000 µg/ml). The antibiotic potentiation activity was studied in combination with seven widely used antibiotics against extremely drug resistant (XDR) *Pseudomonas aeruginosa*. Major reductions in minimum inhibitory concentrations (MIC, 10–14-folds) of the antibiotics meropenem (10 fold) and trimethoprim (14 fold) were observed in the presence of VAuNPs (50 µg/ml). Furthermore, it was found that VAuNPs in combination with meropenem or trimethoprim provided 1.5–3-fold better potentiation effects than that of vanillin alone. Use of an ethidium bromide agar cart wheel assay indicated that VAuNPs can block the activity of efflux pumps. High reduction in the MIC of antibiotics was therefore attributed to the efflux pump repression activity of VAuNPs. Further, RT-qPCR of clinically relevant MexAB-OprM efflux pump components showed down-regulation in *mexB* and *OprM* transcripts in VAuNPs treated *P. aeruginosa* clinical isolates. Our results reveal that VAuNPs impart susceptibility to the last line antibiotics meropenem, trimethoprim and few widely used antibiotics in XDR *P. aeruginosa* clinical isolates that display resistance to these antibiotics. Therefore, this study indicate the ability of VAuNPs and vanillin to be used as antibiotic adjuvants for inhibiting bacterial efflux pumps to potentiate antibiotics for addressing AMR problem affecting human health and environment.

1. Introduction

Pseudomonas aeruginosa is a Gram-negative Gamma-proteobacteria, that causes nosocomial infections in immunocompromised patients suffering from cystic fibrosis, pneumonia and sepsis (Smith et al., 2016). The innate and acquired resistance mechanisms to antibiotics make *P. aeruginosa* a superbug capable of inactivating even the last line of antibiotics (Breidenstein et al., 2011). To compound this, increased antibiotic resistance results in elevated administration of antibiotics to treat extremely drug-resistant (XDR) infections. Hence, the World Health Organisation (WHO) has categorized *P. aeruginosa* as a critical priority bacterium that needs immediate attention (WHO, 2017). Evolution of

antibiotic resistance in such pathogens is outpacing the launch of new antibiotics (Ventola, 2015) and according to the Centers for Disease Control and Prevention Institute (CDC), Atlanta, USA, only six antibiotics have been introduced to the market in the past ~45 years, a fact that reiterates the complexity and seriousness of a potential post-antibiotic era (CDC, 2014).

Antibiotics function by targeting vital cellular mechanisms of bacteria (DNA, RNA, protein and cell wall synthesis). However, due to prolonged and excessive misuse, these are now being neutralized by bacterial resistance mechanisms (Lambert, 2002). In addition to investigating new approaches to target bacterial vital processes with additional therapeutics, targets within the underlying antibiotic resistance mechanisms can

* Corresponding author.

E-mail address: keshari2u@gmail.com (S.K. Lenka).

<https://doi.org/10.1016/j.heliyon.2019.e02021>

Received 30 March 2019; Received in revised form 24 May 2019; Accepted 27 June 2019

2405-8440/© 2019 Published by Elsevier Ltd. This is an open access article under the CC BY-NC-ND license (<http://creativecommons.org/licenses/by-nc-nd/4.0/>).

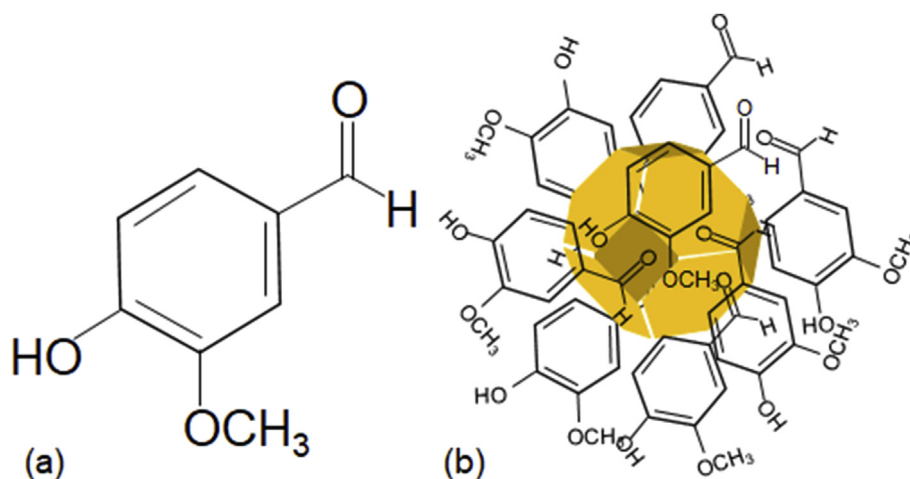


Fig. 1. (a) Chemical structure of vanillin, (b) Predicted structure of vanillin capped gold nanoparticles.

also be explored. Amongst these antibiotic resistance strategies, the most effective approaches are the degradation/modification of antibiotic by enzymes, removal by efflux pumps and exclusion due to increased membrane permeability (Cabot et al., 2016). Although efflux pumps confer low intrinsic resistance towards antibiotics, their overexpression and/or accumulation of mutations in their corresponding genes makes them potential targets for manipulating resistance mechanisms (Poole, 2007). Recently, reports on metallic nanoparticles like Ag, Cu, ZnO and magnetite nanoparticles have surfaced with an ability to potentiate the effect of conventional antibiotics by blocking bacterial efflux pumps (Gupta et al., 2017a, 2017b). Nanoparticles of noble metals (gold and silver) have emerged as potential delivery agents in the therapeutic field for carrying small drug molecule(s), however, gold nanoparticles (AuNPs) are yet to be explored for their antibiotic potentiation and efflux pump inhibition activity.

Recently, AuNPs are under the purview of drug developers due to their surface plasmon resonance, optical and tunable properties. Small phytomolecule(s) delivered by capping onto AuNPs have been reported to have enhanced stability, bioavailability and biocompatibility compared to the carrier alone (Das et al., 2016; Zhao et al., 2010). Various drawbacks in the use of phytochemicals as therapeutic agents are often put forward, for example short half-life, delayed clearance, low specificity and insufficient cell penetration (Singh et al., 2018). Many of these can potentially be addressed by conjugation with AuNPs. For instance, kaempferol conjugated to AuNPs displayed higher apoptosis and anti-angiogenesis activity in MCF-7 breast cancer cells as compared to kaempferol alone (Raghavan et al., 2015). Phytomolecules like curcumin with proven antibiotic potentiation effects can be capped onto AuNPs to get enhanced bioactivity with respect to curcumin alone (Moghaddam et al., 2009; Sindhu et al., 2014). However, curcumin is insoluble in water and degrades into its constituent and stable products which include vanillin and ferulic acid. Interestingly, the bioactivities of curcumin are now attributed to these constituent degradation products (Bezerra et al., 2017; Iannuzzi et al., 2017). Therefore we have chosen vanillin to investigate as an antibiotic potentiating agent.

Vanillin (4-hydroxy-3-methoxybenzaldehyde; Fig. 1a) is the principal and characteristic ingredient of the world's most popular vanilla flavour isolated from *Vanilla planifolia* (Gallage and Møller, 2018). Vanillin has an aromatic ring with different functional groups, which includes aldehyde, hydroxyl and ether. Albeit known for its flavour and fragrance, it also possesses diverse bioactive properties (Bezerra et al., 2016) which include proposed neuroprotective, anti-inflammatory properties, along with H1N1 neuraminidase inhibitory activity (Dhanalakshmi et al., 2016; Edwards et al., 2017; Hariono et al., 2016; Khan et al., 2017). Moreover, vanillin is a Food and Drug Administration (FDA) approved food additive and has been classified with a 'Generally Recognised as

Safe' (GRAS) status by the FDA (<https://www.accessdata.fda.gov/scripts/cdrh/cfdocs/cfcfr/CFRSearch.cfm?fr=182.60>, Accessed - 23/12/2018). In this study, we synthesized vanillin capped gold nanoparticles (VAuNPs) using vanillin as a reducing and capping agent in a one-step synthesis process (Fig. 1b). The production of VAuNPs was done for the purpose of enhancing the bioavailability and bioactivity of vanillin. The VAuNPs were found non-bactericidal even at high concentrations (>2000 µg/ml), and importantly, these were effective in potentiating the activity of antibiotics against XDR *P. aeruginosa* clinical isolates. This study demonstrates the novel usage of VAuNPs and vanillin for making XDR bacteria more susceptible to last line antibiotics such as meropenem and trimethoprim and provides a new approach towards addressing the AMR crisis affecting human health.

2. Materials and methods

2.1. Bacterial strains and chemicals

P. aeruginosa clinical isolates were collected from B. J. Medical Govt. College, Pune, India and Golwilkar Metropolis Pathology Laboratory, Pune, India. These isolates were characterized as XDR and evaluated for the presence of MexAB-OprM efflux pump in our previous study (Arya et al., unpublished). Selected isolates (i.e. PA11 and PA14) used for antibiotic potentiation and RT-qPCR analysis in this study were further identified by 16S ribosomal (rRNA) sequencing. The 16S rRNA sequences were submitted to the GenBank with accession numbers MH748607 and MK077676 for PA11 and PA14 respectively. In addition to PA11 and PA14, isolates with high efflux pump activity, namely PA01, PA03, PA04, PA07, PA09, PA12, & PA13 were taken for phenotypic detection of efflux inhibition activity (Arya et al., unpublished). The clinical isolates were grown in Muller Hinton Broth (MHB) and maintained on Muller Hinton Agar (MHA) plates. Vanillin, chloroauric acid (HAuCl₄), trisodium citrate, ethidium bromide was purchased from Sigma Aldrich, St. Louis, USA and antibiotic powders were purchased from Sigma Aldrich, St. Louis, USA and HiMedia Lab., Mumbai, India.

2.2. Green synthesis and physicochemical characterization of gold nanoparticles

A stock solution of 50 mM vanillin and 100 mM HAuCl₄ were prepared in ultrapure water (Milli-Q; Millipore, GmbH). Formation of vanillin-mediated green synthesized AuNPs was investigated by using varying concentrations of both the reactants (0.25 mM–4 mM vanillin and 1 mM - 2 mM HAuCl₄). The reactions were carried out at room temperature. The effect of reaction time (0–12 h) on synthesis of VAuNPs was investigated with the optimized concentrations of vanillin and

HAuCl₄. Spectrophotometric (UV-2450, Spectrophotometer, Shimadzu, Kyoto, Japan) analysis was performed to investigate the changes in surface plasmon resonance (SPR) of the VAuNPs synthesized at varying concentrations. Morphological details and chemical composition of VAuNPs were analysed by using a transmission electron microscope (TEM) and energy dispersal X-ray spectroscopy (EDX) (FEI Tecnai F20 TEM, Philips, Netherlands). Zeta potential and hydrodynamic size of VAuNPs were analyzed by zeta sizer (Malvern Zetasizer Nano ZS, United Kingdom). Surface capping and crystallinity of VAuNPs were investigated by fourier transform infra-red spectroscopy (FTIR, Perkin-Elmer Norwalk, USA) and X-ray diffraction (XRD, Bruker AXS Inc) respectively.

2.3. Chemically synthesized gold nanoparticles (CSAuNPs)

Gold nanoparticles used as control against VAuNPs were chemically synthesized as per the protocol given by Bastus et al., with some modifications (Bastús et al., 2011). Briefly, a solution of 2.2 mM trisodium citrate in ultrapure water was heated in a 250 ml conical flask for 15 min under vigorous stirring. After boiling, 1 ml of 25 mM HAuCl₄ was mixed to the solution. The solution was heated until a pink colour had formed. Chemically synthesized gold nanoparticles (CSAuNPs) were recovered and characterized by UV-Vis spectroscopy.

2.4. Minimum inhibitory concentration of antibiotics, VAuNPs, vanillin and CSAuNPs

Minimum inhibitory concentration (MIC) of antibiotics (Chloramphenicol-CIP, levofloxacin-LEV, ciprofloxacin-CIP, tigecycline-TGC, meropenem-MRP, trimethoprim-TR and fosfomycin-FOS), vanillin, VAuNPs and CSAuNPs were calculated by a micro-broth dilution assay in 96-well plates (Patel, 2017). Briefly, the wells were inoculated with 10⁶ cells/ml in MHB supplemented with increasing concentration of antibiotics, incubated overnight at 37 °C and the absorbance was measured at λ_{max} = 600 nm. The wells with absorbance values ≤0.01 were considered as non-turbid. Similarly, the MIC was measured for vanillin, VAuNPs and CSAuNPs.

2.5. Checkerboard assay, antibiotic potentiation and fold reduction in MIC

Checkerboard assays were performed to identify the most suitable concentration of VAuNPs and vanillin to be used for antibiotic potentiation experiments (Corbett et al., 2017; Lorenzi et al., 2009; Miladi et al., 2016). For this, a 96-well plate was used, where MHB was added in each well, with increasing concentrations of selected antibiotics in rows and increasing concentration of VAuNPs and vanillin in columns. Wells were then inoculated with a bacterial suspension of 10⁶ cells/ml. These 96-well plates were incubated overnight at 37 °C. On the next day, the MIC of the various combinations (antibiotic + VAuNPs/vanillin) was calculated for primary non-turbid wells (no growth/lowest absorbance) in each column and row of the 96-well plate. This represented the lowest antibiotic and VAuNPs/vanillin combination required to inhibit the growth of *P. aeruginosa* (planktonic cells). Similarly, to evaluate the antibiotics potentiation effect of VAuNPs/vanillin and antibiotics (C, LEV, CIP, TGC, MRP, TR and FOS), MHB supplemented with antibiotics and VAuNPs/vanillin at sub-MIC (50 µg/ml) concentration was inoculated with PA11 and PA14 clinical isolates in 96-well plates as mentioned earlier. The absorbance was recorded after overnight incubation at 37 °C. Likewise, antibiotic potentiation effects of chemically synthesised AuNPs (CSAuNPs) were also evaluated as control for VAuNPs. Antibiotic potentiation experiments were repeated three times.

Fold reduction in MIC of antibiotic was calculated as follows:

$$\text{Fold reduction} = \text{MIC of ABX} / \text{MIC of ABX} + \text{VAuNPs}$$

Similarly, fold reduction was also calculated for vanillin and CSAuNPs.

2.6. Fractional inhibitory concentration (FIC) index

To determine the extent of synergism and combinatorial inhibitory effects of antibiotics and VAuNPs/vanillin/CSAuNPs, the FIC indexes were calculated by the following formula (Berenbaum, 1978; Den Hollander et al., 1998).

$$\text{Fractional inhibitory concentration index: } \sum \text{FIC} = \text{FICA} + \text{FICB}$$

FIC_A = MIC of C_A in combination/MIC of C_A, FIC_B = MIC of C_B in combination/MIC of C_B; where A and B are antibiotics and VAuNPs respectively. FIC index value indicates synergistic (≤0.5), additive (0.5 ≥ 1) and antagonistic (>1) effects of the combinations used.

2.7. Scanning electron microscopy of *P. aeruginosa*

The scanning electron microscopic (SEM) analysis of *P. aeruginosa* (untreated-control, treated-meropenem, VAuNPs and meropenem + VAuNPs) was performed as per Chao and Zhang with some modifications (Chao and Zhang, 2011). Bacteria in exponential growth phase (1 × 10⁸ CFU/ml) were treated as control (a) and the test samples were grown with 50 µg/ml VAuNPs (b) 200 µg/ml meropenem (c) and 50 + 20 µg/ml VAuNPs + meropenem (d). These test samples were incubated for 4 h at 37 °C before centrifuging at 2,000 rpm for 10 min. The cell pellets were washed twice in 0.1 % phosphate buffer saline (PBS) and fixed in ethanol/acetic acid (3:1) for 20 min at room temperature. After fixation, the cells were washed in 0.1 % PBS, centrifuged and resuspended in sterilized ultrapure water for SEM analysis. Sample preparation was done as per Dosunmu et al. and the SEM images were taken on FESEM (Field Emission Scanning Electron Microscope, Nova Nano SEM 450, Thermo Fisher Scientific, Waltham, MA, USA) (Dosunmu et al., 2015).

2.8. Ethidium bromide agar cartwheel assay

Efflux pump inhibition activity of VAuNPs, vanillin and CSAuNPs were also assessed using an Ethidium bromide (EtBr) cartwheel assay. EtBr is a substrate of efflux pumps and therefore used to detect efflux pump activity by EtBr-agar cartwheel assay (Martins et al., 2013). MHA supplemented with a range of EtBr concentrations (0–2.5 µg/ml) were poured in Petri plates. Bacterial strains (10⁶ cells/ml) were streaked in cartwheel pattern on the plates. The plates were incubated overnight at 37 °C and observed under UV for fluorescence (Bio-Rad Gel-Doc XR system, Hercules, CA, USA). Efflux pump inhibition activity of vanillin, VAuNPs and CSAuNPs were also assessed by EtBr cartwheel assay. Briefly, efflux pump active clinical isolates (10⁶ cells/ml) were grown overnight in MHB supplemented in the presence of 50 µg/ml VAuNPs dissolved in ultrapure water. Further, these overnight grown cultures (10⁸ cells/ml) were diluted to 10⁶ cells/ml and treated for 30 min in the same concentration of VAuNPs, vanillin and CSAuNPs separately in MHB. After 30 min of incubation, the cultures were streaked on EtBr and 50 µg/ml vanillin supplemented MHA plates. The same was followed for vanillin and CSAuNPs.

2.9. Expression analysis of MexAB-OprM efflux pump components by RT-qPCR

Expression of *mexB* and *OprM* genes was determined by RT-qPCR as described previously with minor modifications (Mesaros et al., 2007). *P. aeruginosa* clinical isolates (PA11 and PA14) treated with 50 µg/ml of VAuNPs, vanillin and CSAuNPs separately and were grown overnight. After overnight incubation, O.D. of the suspension was adjusted to 0.5 McFarland standard and was followed by total RNA extraction using HiPurA™ Total RNA Purification Kit (HiMedia Lab, Mumbai, India). cDNA was prepared from mRNA (500 ng) using Hi-cDNA Synthesis Kit (HiMedia Lab, Mumbai, India) and was subjected to RT-qPCR. MexAB-OprM mRNA transcription level was evaluated using Hi-SYBr Master

Table 1
Primers used for MexAB-OprM efflux pump expression analysis.

Name	Sequence	Reference
MexB-F	5'-GTGTTCCGGCTCGCAGTACTC-3'	(Yoneda et al., 2005)
MexB-R	5'-AACCGTCGGGATTGACCTTG-3'	(Yoneda et al., 2005)
OprM-F	5'-CCATGAGCCGCCAACTGTC-3'	(Savli et al., 2003)
OprM-R	5'-CCTGGAACGCCGTCTGGAT-3'	(Savli et al., 2003)
rpsL-F	5'-GCAACTATCAACCAGCTGGTG-3'	(Llanes et al., 2004)
rpsL-R	5'-GCTGTCTCTTGCAGGTTGTG-3'	(Llanes et al., 2004)

Mix (HiMedia Lab, Mumbai, India). MexAB-OprM pump specific primers were used for expression analysis (Table 1) (Llanes et al., 2004; Savli et al., 2003; Yoneda et al., 2005). The fold-change in expression of MexAB-OprM pump components between any two samples was calculated using the $2^{-\Delta\Delta Ct}$ method (Schmittgen and Livak, 2008). To normalize the transcriptional level of target genes, expression of the *rpsL* gene (30S ribosomal gene) was also determined and calibrated against corresponding mRNA expression. The experiments were performed with two technical replicates.

2.10. Statistical analysis

The synthesis and characterization experiments of VAuNPs were performed in triplicates. The potentiation studies were performed twice, with each treatment conducted in triplicate. One-way ANOVA was used

for statistical significance and a p-value < 0.05 was regarded as significant. Gene expression studies - data are shown as mean average with error bars representing standard error.

3. Results and discussion

3.1. Green synthesis and physicochemical characterization of gold nanoparticles

The synthesis of VAuNPs at room temperature was performed by reducing 1 mM and 2 mM HAuCl₄ solution with different concentrations of vanillin (0.25 mM - 4 mM) (Fig. 2a). UV-Vis spectra originating from the optoelectronic property SPR confirmed the synthesis of VAuNPs. A SPR peak centred at around 560 nm was observed for 2 mM HAuCl₄ + 1 mM vanillin concentration. For lower concentrations of vanillin and 1 mM HAuCl₄, SPR peaks were either absent or very broad (Data not shown). Higher concentrations (2 mM and 4 mM) of vanillin displayed broader SPR peaks with bathochromic shift. Thus, 2 mM HAuCl₄ + 1 mM vanillin was considered as optimum concentrations for the synthesis of VAuNPs (Fig. 2c). Reaction time optimization of this combination showed no change in the SPR band intensity after more than 3 h of incubation (Fig. 2b). Hence, 3 h reaction time was considered to be the optimum and was used for bulk synthesis in this study.

TEM and EDX analysis of VAuNPs synthesized from 2 mM HAuCl₄ + 1 mM vanillin revealed the morphological and elemental details. VAuNPs

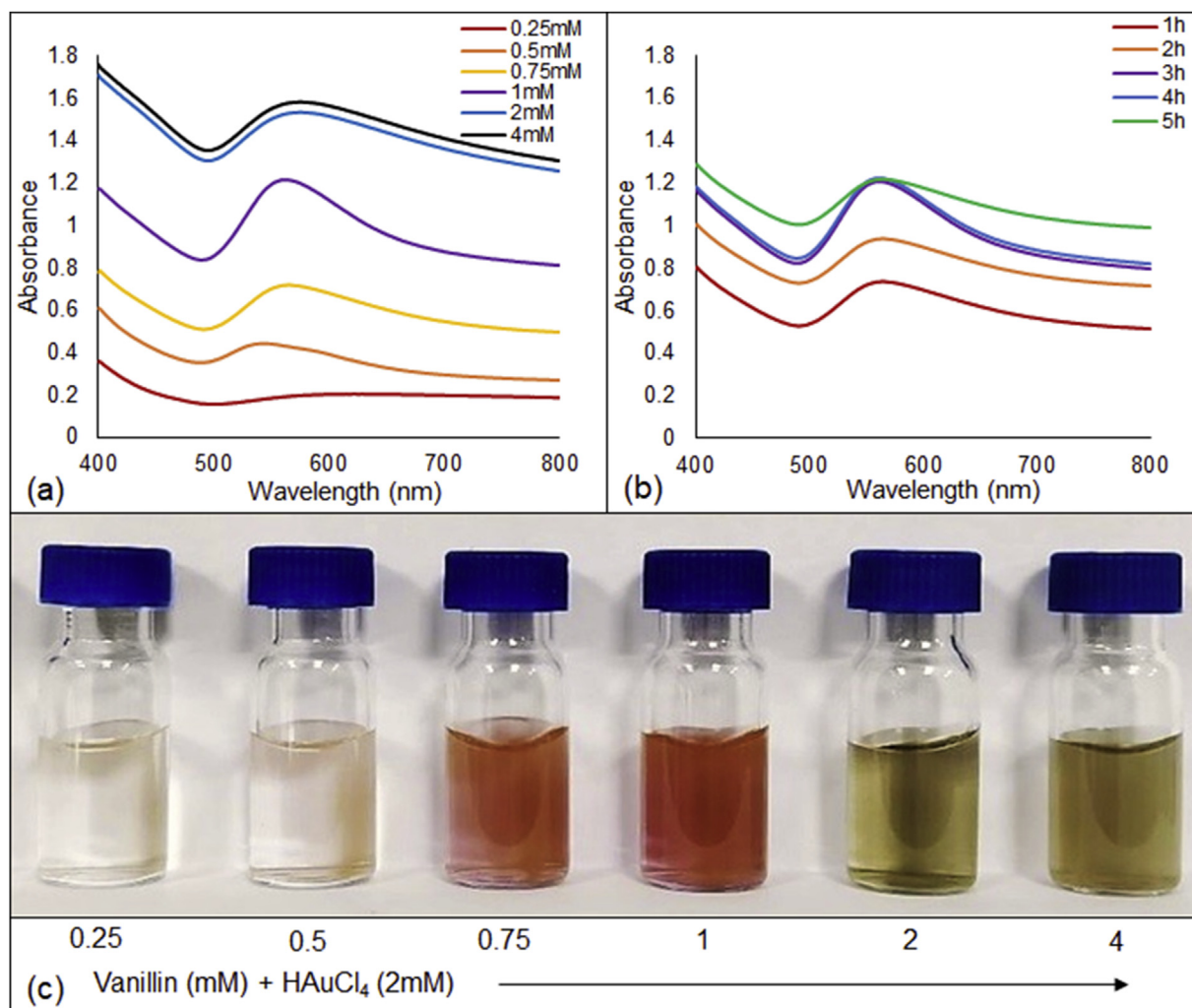


Fig. 2. UV-Vis spectra of VAuNPs synthesized by reacting 2 mM of HAuCl₄ with (a) different concentration of vanillin (0.25–4 mM) (b) different time of incubation and (c) SPR of VAuNPs.

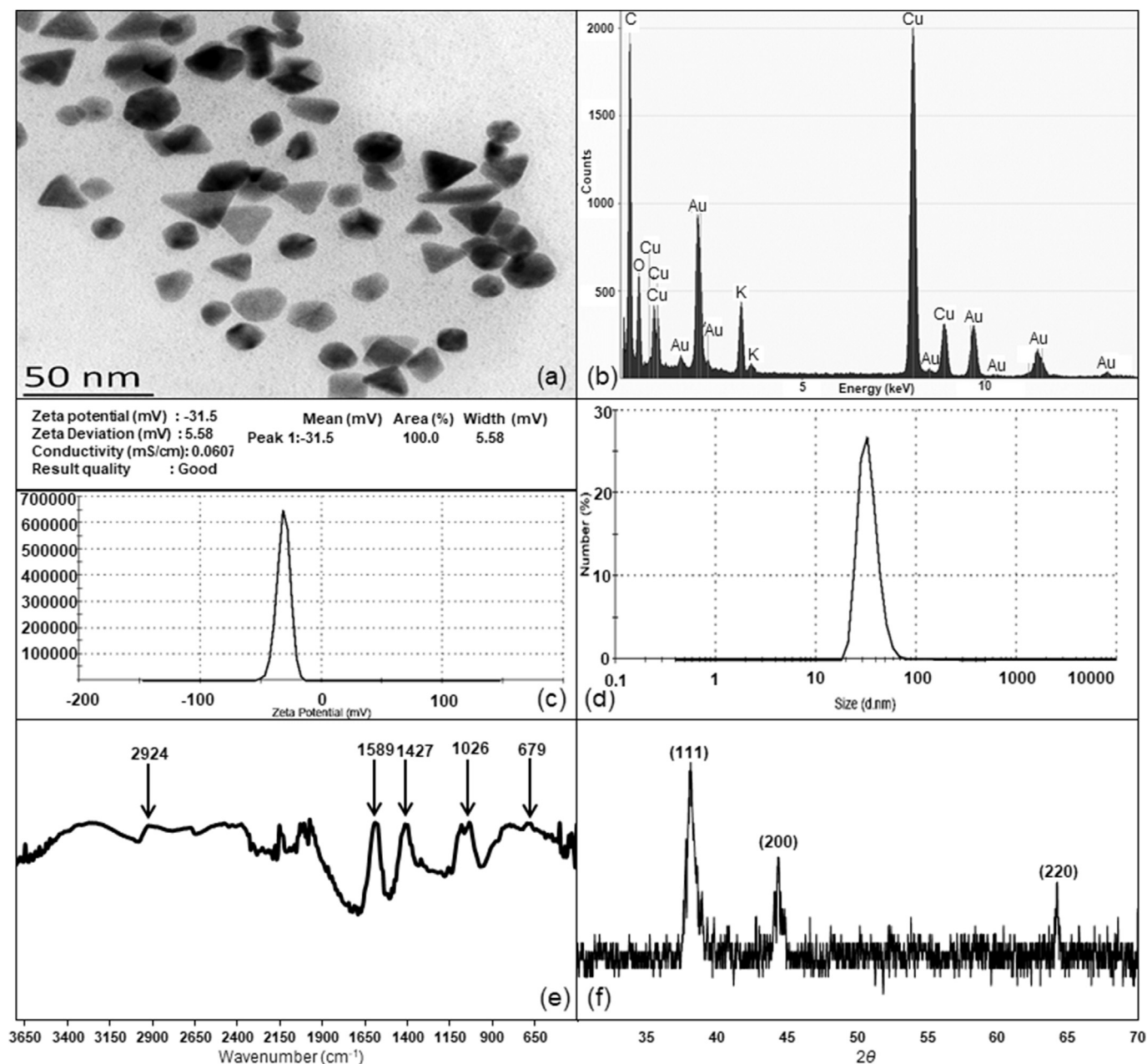


Fig. 3. Characterization of VAuNPs: (a) Transmission electron micrograph (Size - 20–30 nm), (b) Energy dispersive X-ray spectroscopy (Presence of Au, C and O), (c) Zeta potential (-31.5), (d) Size distribution (Average size - 35 nm), (e) FTIR spectra, (f) X-ray diffraction pattern.

were predominantly of hexagonal, triangular and spherical shapes (Fig. 3a). As expected, the EDX analysis showed the presence of gold, carbon and oxygen (Fig. 3b). The zeta potential and average size of the synthesized VAuNPs were found to be -31.5 mV and 35 nm, respectively (Fig. 3c and d). A low polydispersity index (PDI) value (0.376) indicated high particle homogeneity. A size range of below 100 nm indicated dimensional correctness; while high zeta potentials assured stability of the VAuNPs. FTIR prominent peaks were observed at 2924 cm^{-1} , 1589 cm^{-1} , 1427 cm^{-1} , 1026 cm^{-1} and 679 cm^{-1} (Fig. 3e). FTIR-ATR analysis of VAuNPs showed the presence of different functional groups originating from the vanillin molecules capped on the surfaces of VAuNPs. FTIR peaks observed at 2924 cm^{-1} , 1589 cm^{-1} , 1427 cm^{-1} , 1026 cm^{-1} and 679 cm^{-1} correspond to stretching vibrations of C–H, stretching vibrations of C=C–C group, stretching vibrations of O–CH₃ and bending vibration of C=O, respectively (Fatoni et al., 2018).

XRD spectrum of VAuNPs displayed three Bragg reflections at 38.2°,

44.4° and 64.2° 2θ angles. These reflections were indexed on the basis of face-centered cubic (fcc) gold structure corresponding to (111) (200) and (220) confirming the synthesis of crystalline AuNPs (Fig. 3f). CSAuNPs synthesized by reducing HAuCl₄ with trisodium citrate displayed SPR band with a peak centred at 530 nm.

Surface capping of AuNPs with vanillin was well supported by EDX, FTIR and bioactivity studies. Moreover, literature on AuNPs coated with organic molecules such as curcumin also supports our findings, for example, a recent report on curcumin functionalized gold nanoparticles have hypothesized that di-carbonyl moieties of curcumin play a role in reducing Au³⁺ ions and subsequent capping of curcumin (Sindhu et al., 2014). This result was further supported by time-dependent density functional theory and antioxidant assay, where the carbonyl moieties in curcumin displayed a crucial role in reducing Au³⁺ ions to form curcumin capped AuNPs (Singh et al., 2013). Similarly, vanillin has one reactive carbonyl moiety and is prone to attack by various reagents, notably

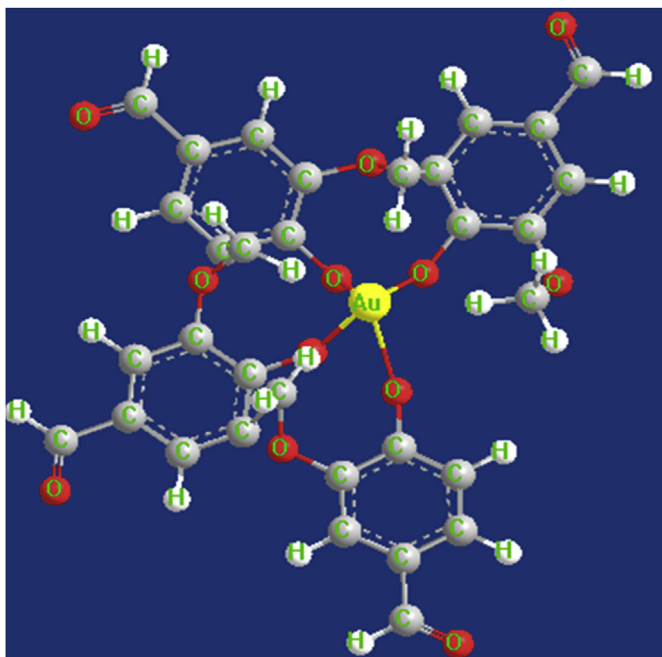


Fig. 4. Surface capping of gold nanoparticles with vanillin. Predicted reduction of Au^{3+} carbonyl moiety of vanillin. Reactive carbonyl moiety of vanillin interacts with Au ion and reduces it to form VAuNPs.

nucleophiles (Frenkel and Havkin-Frenkel, 2006). Relating our present findings with the available literature, it can be hypothesized that the carbonyl moiety in vanillin reduces Au^{3+} ions to form vanillin capped AuNPs. Fig. 4 showcases the most stable conformation of vanillin and possible reduction of Au^{3+} with carbonyl moiety of vanillin (Balachandran and Parimala, 2012).

3.2. Evaluation of MIC and checkerboard assay

The MIC concentration of VAuNPs, vanillin, and CSAuNPs against selected cultures (PA11 and PA14) was found to be $> 2000 \mu\text{g/ml}$. Checkerboard assays were performed to evaluate individual and combined MIC of antibiotics and sub-MIC of VAuNPs. Meropenem and ciprofloxacin were chosen to perform checkerboard assay and finalize the sub-MIC of VAuNPs and vanillin for potentiation studies. Out of various concentrations tested, $50 \mu\text{g/ml}$ concentration of VAuNPs and vanillin was chosen for potentiation studies (Fig. 5a and b). Subsequently, the same concentration of VAuNPs, vanillin and CSAuNPs (i.e. $50 \mu\text{g/ml}$) was used for further efflux pump inhibition and RT-qPCR studies.

Phytochemicals are classified as bactericidal if the MIC ranges in between 100 to $1000 \mu\text{g/ml}$ (Simoes et al., 2009). A high MIC of vanillin and VAuNPs i.e. $2000 \mu\text{g/ml}$ supports a previous study into the antibiotic modulatory activity of vanillin (Bezerra et al., 2017). Therefore, due to non-bactericidal properties of VAuNPs and vanillin, they were further assessed for antibiotic potentiation activity at sub-MIC concentrations.

3.3. Antibiotic potentiation, fold change in minimum inhibitory concentration and FIC index

The checkerboard assay was performed for the antibiotic potentiation studies. The VAuNPs and vanillin treated cultures showed reduction in the MIC values of almost all the antibiotics used as compared to the CSAuNPs treated and control PA11 and PA14 strains. In case of PA11, the difference between MIC of VAuNPs + trimethoprim was up to 3-fold more than that of vanillin + trimethoprim and 10–14-fold more for VAuNPs + meropenem/trimethoprim as compared to the control. In case

of PA14, VAuNPs and vanillin potentiated the activity of trimethoprim by 3–4.8-fold as compared to the control, however, no potentiation was observed for meropenem. Overall, VAuNPs and vanillin showed significant antibiotic potentiation against most of the antibiotics i.e. C, LEV, CIP, C, TGC, MRP, TR, FOS as compared to control and CSAuNPs treated strains (Table 2; Fig. 5c and d). Moreover, the antibiotic potentiation obtained with VAuNPs was significantly better than that of vanillin, i.e. for C, TGC, MRP, TR in case of PA11 and C, CIP, TGC, TR in case of PA14. However, no significant difference was observed in the antibiotic potentiation effects of vanillin and VAuNPs for LEV and FOS in case of both PA11 and PA14 strains. In addition to the above findings, CSAuNPs also showed slight potentiation of C and TR in both PA11 and PA14 strains.

We demonstrated that VAuNPs and vanillin can potentiate the activity of C, LEV, CIP, TGC, and FOS; however, highest MIC reduction of 10–14-fold was observed for VAuNPs + MRP and TR against PA11 clinical isolate. In a similar study it was demonstrated that vanillin can selectively modulate the activity of antibiotics namely, gentamycin, imipenem, norfloxacin, tetracycline and erythromycin against selected gamma-proteobacteria (Bezerra et al., 2017). Through our study we showed that vanillin can further potentiate the activities of C, LEV, CIP, TGC, MRP, TR and FOS as well (Fig. 5c and d). Most importantly, VAuNPs and vanillin could restore the activities of last line antibiotics like MRP and TR to which PA11 was initially resistant (Avrain et al., 2013; Bryan, 2018).

The FIC index of VAuNPs and vanillin with the antibiotics used showed synergism except for FOS (Table 2). VAuNPs and vanillin showed synergistic activity with C, LEV, CIP, TGC, MRP and TR. A similar trend was seen for vanillin in combination with norfloxacin belonging to fluoroquinolones against *P. aeruginosa* and imipenem belonging to carbapenems against *Staphylococcus aureus* (Bezerra et al., 2017). However, through the FIC index we can conclude that synergistic effect of VAuNPs with antibiotics was superior to that of vanillin with antibiotics (as shown in Table 2).

3.4. SEM analysis of ABX and VAuNPs treated *P. aeruginosa*

Scanning electron microscopy was performed for control, VAuNPs, meropenem and VAuNPs + meropenem treated *P. aeruginosa* (PA11) (Fig. 6). Control bacteria and those treated with VAuNPs ($50 \mu\text{g/ml}$) showed no detectable morphological change (Fig. 6a and b), in contrast, those subjected to $200 \mu\text{g/ml}$ of meropenem or even $50 \mu\text{g/ml}$ of VAuNPs along with $20 \mu\text{g/ml}$ of meropenem where both of these treatment groups displayed damaged cells (Fig. 6c and d). Importantly, Fig. 6c and b both show similar cell damage indicating VAuNP's antibiotic potentiation activity, as a similar level of damage can be viewed at a much lower concentration of meropenem due to the presence of VAuNP (as was also shown in Fig. 5c).

3.5. Phenotypic detection of efflux inhibition by EtBr agar cart wheel assay and expression analysis of MexAB-OprM efflux pump components by RT-qPCR

As >4 -fold reduction in MIC of antibiotics in presence of potentiating agent is considered an attribute of efflux pump inhibition, a phenotypic assessment of efflux pump inhibition was performed (Azimi et al., 2016). Efflux pump active *P. aeruginosa* cultures from our previous study (isolates PA01, PA03, PA04, PA07, PA09, PA12, & PA13), in addition to PA11 and PA14 used in the current study were selected to examine efflux inhibitory activity of vanillin and VAuNPs (Arya et al., unpublished). EtBr-agar cartwheel assay of control (untreated and $50 \mu\text{g/ml}$; CSAuNPs) and treated ($50 \mu\text{g/ml}$; vanillin and VAuNPs) cultures showed fluorescence in treated cultures as compared to the respective controls (Fig. 7).

Multiple approaches have been enlisted in order to inhibit or bypass efflux pump activity, specifically by repressing the expression of efflux pump genes, disrupt pump assembly, block outer membrane channels

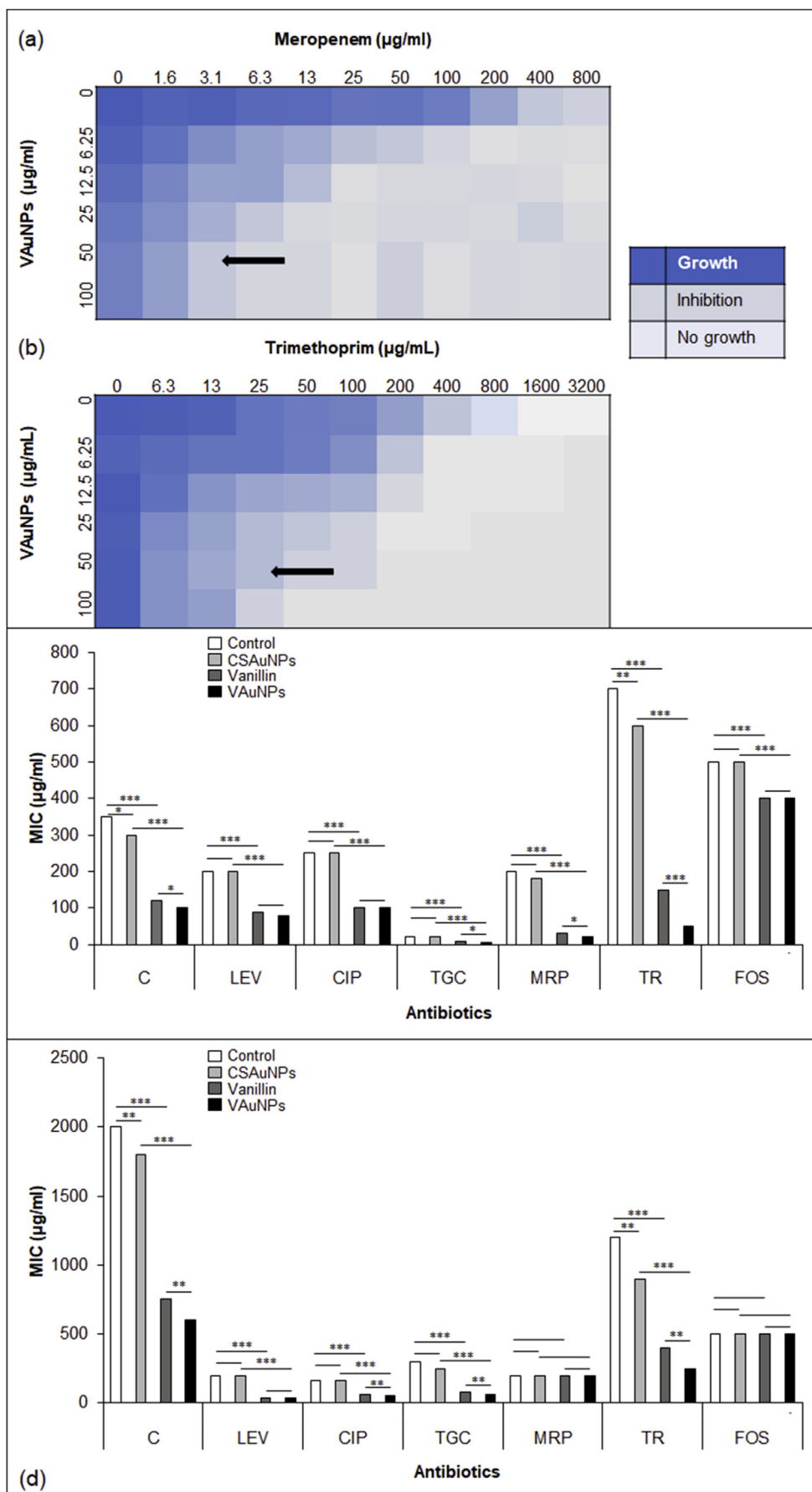


Fig. 5. Checker board assay for PA11 (a) Meropenem and VAuNPs, (b) Trimethoprim and VAuNPs. Arrow indicates the optimum concentration of VAuNPs identified for potentiation experiments. The darkness of blue is representative of the level of growth. Antibiotic potentiation against (c) PA11 and (d) PA14 with CSAuNPs, vanillin and VAuNPs, were CSAuNPs are used as control for VAuNPs. The tested antibiotics were chloramphenicol (C), levofloxacin (LEV), ciprofloxacin (CIP), tigecycline (TGC), meropenem (MRP), trimethoprim (TR), Fosfomycin (FOS). Reduction in MIC was observed for all the antibiotics. ≥ 10 -fold reduction was seen for MRP and TR. One-way ANOVA was used for statistical significance where, *p-value < 0.05, **p-value < 0.01, ***p-value < 0.001. (VAuNPs-Vanillin capped gold nanoparticles; CSAuNPs-Chemically synthesized gold nanoparticles).

Table 2

Fold reduction in MIC and FIC index of selected antibiotics in combination with VAuNPs, vanillin and CSAuNPs treated XDR PA11 and PA14.

Fold change in the minimum inhibitory concentration of antibiotics						
Antibiotics	XDR <i>Pseudomonas aeruginosa</i> clinical isolates					
	PA11				PA14	
	CSAuNPs	Vanillin	VAuNPs	CSAuNPs	Vanillin	VAuNPs
Chloramphenicol	1.2	2.3	3.5	1.11	2.6	3.33
Levofloxacin	1	2	2.5	1	5	5
Ciprofloxacin	1	2.5	2.5	1	2.66	3.2
Tigecycline	1	2	4	1.2	3.7	5
Meropenem	1.11	6.6	10	1	1	1
Trimethoprim	1.16	4.6	14	1.33	3	4.8
Fosfomycin	1	1.2	1.2	1	1	1

Fractional inhibitory concentration index for synergetic activity						
Antibiotics	XDR <i>Pseudomonas aeruginosa</i> clinical isolates					
	PA11				PA14	
	CSAuNPs	Vanillin	VAuNPs	CSAuNPs	Vanillin	VAuNPs
Chloramphenicol	0.88	0.43	0.38	0.93	0.45	0.34
Levofloxacin	1.03	0.48	0.44	1.03	0.24	0.24
Ciprofloxacin	1.03	0.44	0.44	1.03	0.41	0.35
Tigecycline	1.03	0.43	0.29	0.86	0.29	0.24
Meropenem	0.93	0.18	0.11	1.03	1.03	1.03
Trimethoprim	0.89	0.25	0.11	0.78	0.36	0.25
Fosfomycin	1.03	0.83	0.83	1.03	1.03	1.03

Fold reduction – Highlighted values indicates the difference between VAuNPs and vanillin.

$FIC_A = MIC\ of\ C_A\ in\ combination / MIC\ of\ C_A$, $FIC_B = MIC\ of\ C_B\ in\ combination / MIC\ of\ C_B$; where A and B are antibiotics and VAuNPs/vanillin/CSAuNPs respectively. FIC index value indicates synergistic (≤ 0.5), additive ($0.5 \geq 1$) and antagonistic (> 1) effects of the combinations used.

(OprM), competitive inhibition of efflux affinity sites and alteration of the chemical structure of antibiotics that are substrates of efflux pumps (Venter et al., 2015). Expression analysis of MexAB-OprM efflux pump components was conducted with vanillin and VAuNPs treated PA11 and PA14 clinical strains. CSAuNPs treatment was used as a control for VAuNPs. RT-qPCR analysis showed a reduction in the expression of *mexB* and *oprM* genes. VAuNPs treatment showed repression of *mexB* and *oprM* by 3.37 and 6.54-fold respectively, and vanillin treated PA11 showed repression of *mexB* and *oprM* genes which was 1.93 and 2.32-fold respectively (Fig. 8a). Similar response trends were observed in PA14 as well. VAuNPs treatment showed repressions of *mexB* and *oprM* by 2.31

and 5.96-fold respectively; whereas, vanillin treated PA14 showed repression of *mexB* and *oprM* by 2.56 and 2.54-fold respectively (Fig. 8b). Noteworthy is the repression of *OprM* component, which is 2.34–2.81-folds higher than observed in vanillin treated isolates. The outcome of RT-qPCR data supports the previous claims of using AuNPs to enhance the bioactivities of phytochemicals capped on them (Raghavan et al., 2015). While the widely used RT-qPCR technique has the benefit of being quick and sensitive and could be easily applied in clinical laboratory conditions (Dumas et al., 2006), further analysis of MexAB-OprM at the protein level would help verify these observed reductions in gene expression and regulation.

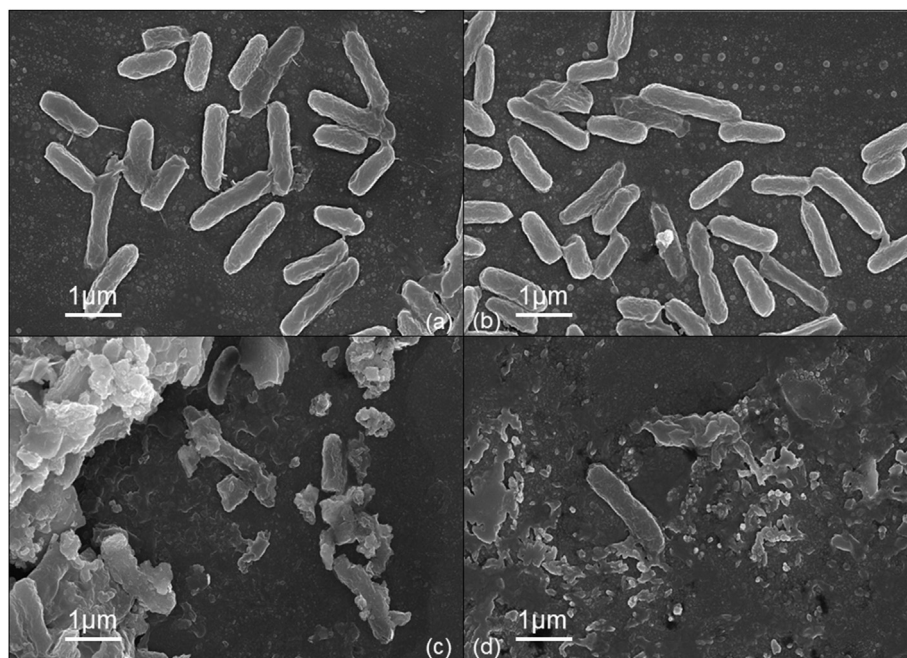


Fig. 6. SEM of *P. aeruginosa* (PA11): (a) untreated, (b) treated with VAuNPs- 50 µg/ml, (c) Meropenem- 200 µg/ml, (d) Meropenem and VAuNPs (20 µg/ml and 50 µg/ml respectively), demonstrating that the addition of VAuNPs reduced the MIC of meropenem by 10-fold.

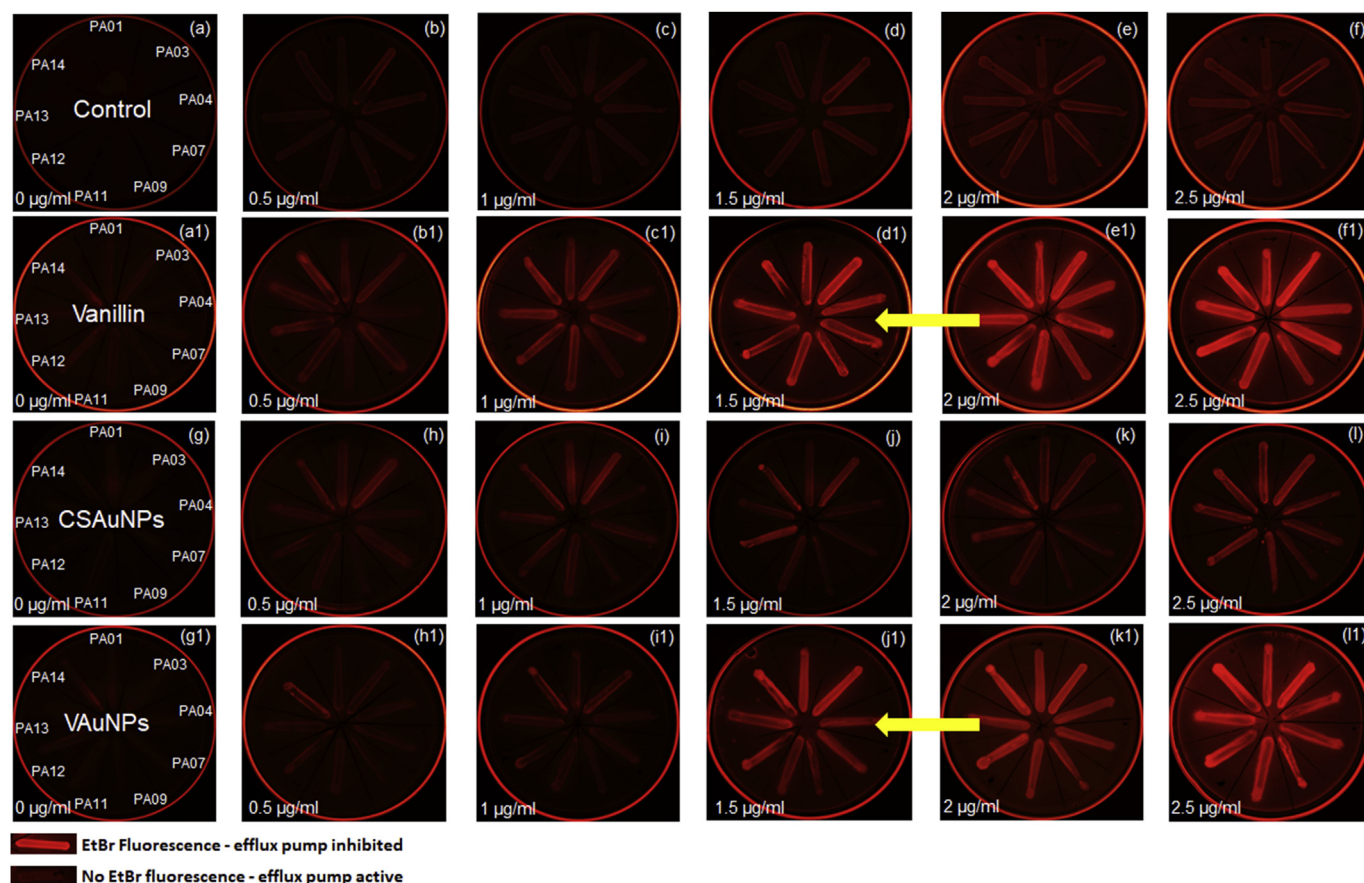


Fig. 7. EtBr cartwheel assay of efflux pump overexpressing XDR *P. aeruginosa* clinical isolates (PA01, PA03, PA04, PA07, PA09, PA11, PA12, PA13 and PA14) streaked on plates with increasing concentrations of EtBr (0–2.5 µg/ml). (a,b,c,d,e,f) Control untreated cultures displaying high efflux activity (a1,b1,c1,d1,e1,f1) 50 µg/ml Vanillin treated cultures showing fluorescence from 1.5 µg/ml EtBr concentration displays possible efflux inhibitory effects produced by vanillin. (g,h,i,j,k,l) CSAuNPs treated cultures displaying no fluorescence in contrast to (g1,h1,i1,j1,k1,l1) VAuNPs treated cultures which showed increased fluorescence from 1.5 µg/ml EtBr concentration. The efflux pump active clinical isolates were streaked in the same orientation as described in the left column. (Arrow indicates the reduced MIC of EtBr in the VAuNPs and Vanillin treated clinical isolates).

Efflux pumps are known to expel multiple classes of antibiotics from the bacterial cells. *P. aeruginosa* is known to express multiple efflux pumps, however amongst those, MexAB-OprM is a clinically relevant efflux pump and has highest antibiotic substrate specificity (Pidcock, 2006). Hence, designing efflux pump inhibitors (EPIs) against this pump can restore the activities of several antibiotics. Recent research are directed toward using nanoparticles and phytomolecule(s) as EPIs (Stavri et al., 2006; Tegos et al., 2002). Various nanoparticles such as Ag, Cu and ZnO and phytomolecules like curcumin, geraniol, conessine and daidzein are reported to have efflux pump inhibitory activity and are also known to rejuvenate bactericidal effects of conventional antibiotics (Gupta et al., 2017b; Kaur et al., 2018; Lorenzi et al., 2009; Siriyong et al., 2017). In a preliminary study, copper nanoparticles demonstrated efflux pump inhibitory effects in MDR *S. aureus* and *P. aeruginosa* (Christena et al., 2015). To date, only one report is available on modulatory effects of silver nanoparticles on AcrB and TolC protein expression (components of the AcrAB-TolC efflux pump) in MDR *Enterobacter cloacae* (Mishra et al., 2018). Reports on antibacterial gold nanoparticles capped with different molecules has been reviewed by Zhao and Jiang (2013). However, as observed for antibiotics, such attempts of employing antibacterial AuNPs will result in development of more resistant bacteria. Thus, our study using non-bactericidal VAuNPs is the first report on employing AuNPs for restoring the activity of antibiotics by efflux pump inhibition. In addition, our findings of vanillin mediated efflux inhibition activities support similar reports on other small phytomolecules like capsaicin, curcumin, thymol, carvacrol, berberine and palmitate (Aghayan et al., 2017; Kalia et al., 2012; Miladi et al., 2016; Negi et al., 2014). Recently, it was also

found that vanillin enhanced the internalization of spectinomycin into MDR *Escherichia coli* cells (Brochado et al., 2018). However, our study provides further details into vanillin mediated antibiotic potentiation and also its efflux inhibitory potential. This supports the previous claims of using gold nanoparticles to increase the drug target specificity, clearance and cell penetration of phytomolecules, which in this case might be operational for vanillin (Singh et al., 2018).

4. Conclusion

In this study, we demonstrated the one-step synthesis of stable and crystalline VAuNPs by using vanillin as a reducing and capping agent. Through antibiotic potentiation studies we also found that VAuNPs can restore the activities of last line antibiotics such as meropenem and trimethoprim. The antibiotic potentiation activity of VAuNPs was found to be stronger than that of vanillin. We also observed that VAuNPs and vanillin can suppress the expression of MexAB-OprM efflux pump genes. Thus, the antibiotic potentiation effect may be attributed to the efflux pump inhibitory activity shown by VAuNPs and vanillin. There is the possibility that VAuNPs and vanillin may also affect other resistance mechanisms; therefore, further analysis of other AMR mechanisms is needed to evaluate the effect of VAuNPs and vanillin on these. However, for the current outcome we can conclude that, VAuNPs and vanillin act as efflux pump inhibitors and restore the activities of last line antibiotics against XDR *P. aeruginosa* clinical isolates.

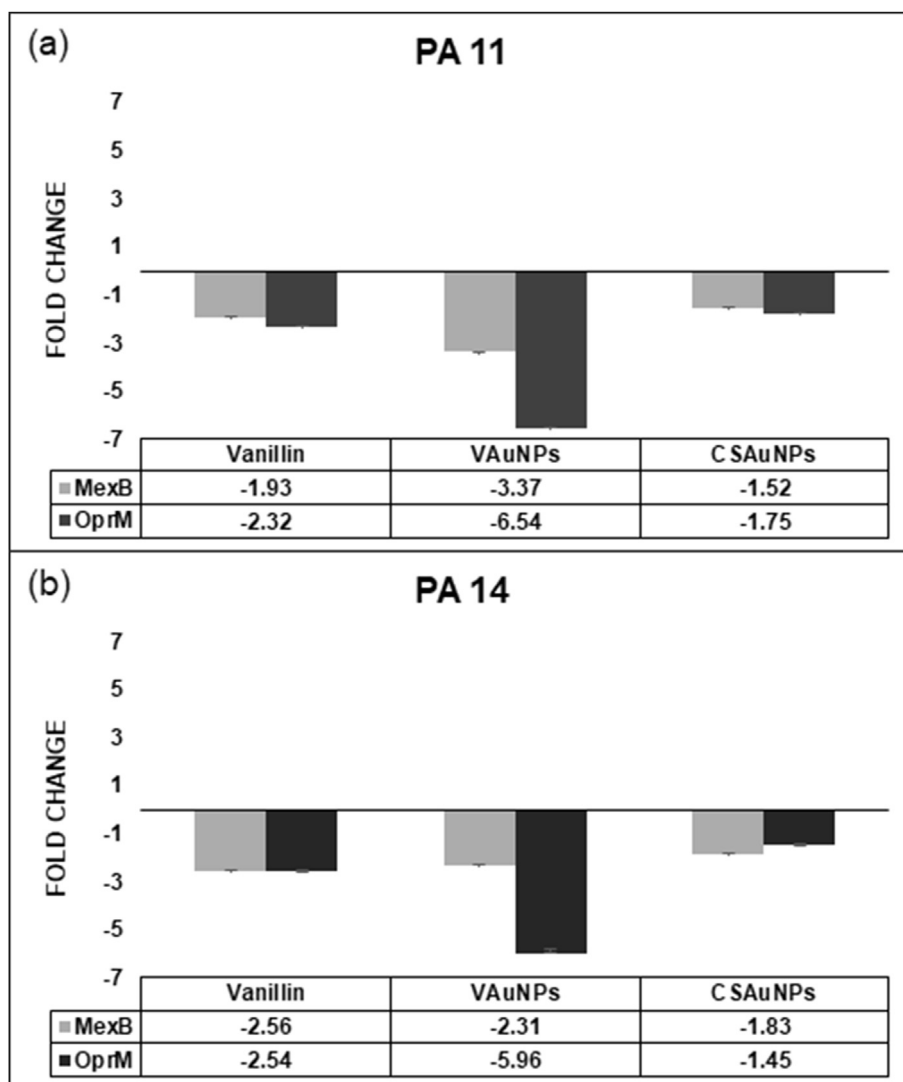


Fig. 8. RT-qPCR analysis of MexAB-OprM efflux pump genes in vanillin, VAuNPs and CSAuNPs treated *P. aeruginosa* clinical isolates (a) PA11 and (b) PA14. CSAuNPs treatment was used as a control for VAuNPs. VAuNPs treatment showed better repression of *mexB* and *oprM* genes as compared to that of vanillin. Data below bars represent the fold change in gene expression compared to the controls. (Data are shown as mean average with error bars representing standard error).

Declarations

Author contribution statement

Sagar Arya: Conceived and designed the experiments; Performed the experiments; Analyzed and interpreted the data; Contributed reagents, materials, analysis tools or data; Wrote the paper.

Mansi Sharma: Performed the experiments; Analyzed and interpreted the data; Contributed reagents, materials, analysis tools or data.

Ratul Kumar Das, Jim Rookes, David Cahill: Analyzed and interpreted the data; Wrote the paper.

Sangram Lenka: Conceived and designed the experiments; Analyzed and interpreted the data; Contributed reagents, materials, analysis tools or data; Wrote the paper.

Funding statement

Sagar Arya is the recipient of a Deakin University, Australia post graduate scholarship.

Competing interest statement

The authors declare the following conflict of interests: two patent applications have been filed with the Indian patent office based on this work: Patent 1 - Application no.: IN 2018 1104 1967 Patent 2 - Application no.: IN 2018 1104 1968.

Additional information

No additional information is available for this paper.

Acknowledgements

The clinical isolates are the courtesy of Dr. Renu Bharadwaj, Head of Department, Microbiology, B. J. Govt. Medical College, Pune – 411001, India and Golwilkar Metropolis Health Services India, Pvt. Ltd., Pune – 411004, India.

References

Aghayan, S.S., Mogadam, H.K., Fazli, M., Darban-Sarokhalil, D., Khoramrooz, S.S., Jabalameli, F., et al., 2017. The effects of berberine and palmartine on efflux pumps

- inhibition with different gene patterns in *Pseudomonas Aeruginosa* isolated from burn infections. *Avicenna J. Med. Biotechnol. (AJMB)* 9, 2.
- Avrain, L., Mertens, P., Van Bambeke, F., 2013. RND efflux pumps in *P. aeruginosa*: an underestimated resistance mechanism. *Antibiot. Susceptibility* 26321, 26–28.
- Azimi, L., Namvar, A.E., Lari, A.R., Jamali, S., Lari, A.R., 2016. Comparison of efflux pump involvement in antibiotic resistance among *Pseudomonas aeruginosa* isolates of burn and non-burn patients. *Arch. Pediatr. Infect. Dis.* 4.
- Balachandran, V., Parimala, K., 2012. Vanillin and isovanillin: comparative vibrational spectroscopic studies, conformational stability and NLO properties by density functional theory calculations. *Spectrochim. Acta Mol. Biomol. Spectrosc.* 95, 354–368.
- Bastús, N.G., Comenge, J., Puentes, V., 2011. Kinetically controlled seeded growth synthesis of citrate-stabilized gold nanoparticles of up to 200 nm: size focusing versus Ostwald ripening. *Langmuir* 27, 11098–11105.
- Berenbaum, M., 1978. A method for testing for synergy with any number of agents. *J. Infect. Dis.* 137, 122–130.
- Bezerra, C.F., Camilo, C.J., do Nascimento Silva, M.K., de Freitas, T.S., Ribeiro-Filho, J., Coutinho, H.D.M., 2017. Vanillin selectively modulates the action of antibiotics against resistant bacteria. *Microb. Pathog.* 113, 265–268.
- Bezerra, D.P., Soares, A.K.N., de Sousa, D.P., 2016. Overview of the role of vanillin on redox status and cancer development. *Oxidative medicine and cellular longevity* 2016.
- Breidenstein, E.B., de la Fuente-Núñez, C., Hancock, R.E., 2011. *Pseudomonas aeruginosa*: all roads lead to resistance. *Trends Microbiol.* 19, 419–426.
- Brochado, A.R., Telzerow, A., Bobonis, J., Banzhaf, M., Mateus, A., Selkig, J., et al., 2018. Species-specific activity of antibacterial drug combinations. *Nature* 559, 259.
- Bryan, J., 2018. Carapenems have stood the test of time so far but resistance is emerging. *Lung Cancer* 15, 05.
- Cabot, G., Zamorano, L., Moyá, B., Juan, C., Navas, A., Blázquez, J., et al., 2016. Evolution of *Pseudomonas aeruginosa* antimicrobial resistance and fitness under low and high mutation supply rates. *Antimicrob. Agents Chemother.* 60 (3), 1767–1778.
- CDC, 2014. Antibiotic Resistance Threats in the United States, 2013. CDC, Atlanta, 2013.
- Chao, Y., Zhang, T., 2011. Optimization of fixation methods for observation of bacterial cell morphology and surface ultrastructures by atomic force microscopy. *Appl. Microbiol. Biotechnol.* 92, 381.
- Christena, L.R., Mangalagowri, V., Pradheeba, P., Ahmed, K.B.A., Shalini, B.I.S., Vidyalakshmi, M., et al., 2015. Copper nanoparticles as an efflux pump inhibitor to tackle drug resistant bacteria. *RSC Adv.* 5, 12899–12909.
- Corbett, D., Wise, A., Langley, T., Skinner, K., Trimby, E., Birchall, S., et al., 2017. Potentiation of antibiotic activity by a novel cationic peptide: potency and spectrum of activity of SPR741. *Antimicrob. Agents Chemother.* 61 (8), e00200–e00217.
- Das, R.K., Brar, S.K., Verma, M., 2016. Checking the biocompatibility of plant-derived metallic nanoparticles: molecular perspectives. *Trends Biotechnol.* 34, 440–449.
- Den Hollander, J.G., Mouton, J.W., Verbrugh, H.A., 1998. Use of pharmacodynamic parameters to predict efficacy of combination therapy by using fractional inhibitory concentration kinetics. *Antimicrob. Agents Chemother.* 42, 744–748.
- Dhanalakshmi, C., Janakiraman, U., Manivasagam, T., Thenmozhi, A.J., Essa, M.M., Kalandar, A., et al., 2016. Vanillin attenuated behavioural impairments, neurochemical deficits, oxidative stress and apoptosis against rotenone induced rat model of Parkinson's disease. *Neurochem. Res.* 41, 1899–1910.
- Dosunmu, E., Chaudhari, A.A., Singh, S.R., Dennis, V.A., Pillai, S.R., 2015. Silver-coated carbon nanotubes downregulate the expression of *Pseudomonas aeruginosa* virulence genes: a potential mechanism for their antimicrobial effect. *Int. J. Nanomed.* 10, 5025.
- Dumas, J.-L., Van Delden, C., Perron, K., Köhler, T., 2006. Analysis of antibiotic resistance gene expression in *Pseudomonas aeruginosa* by quantitative real-time-PCR. *FEMS Microbiol. Lett.* 254, 217–225.
- Edwards, R.L., Luis, P.B., Varuzza, P.V., Joseph, A.I., Presley, S.H., Chaturvedi, R., et al., 2017. The anti-inflammatory activity of curcumin is mediated by its oxidative metabolites. *J. Biol. Chem.* 292 (52), 21243–21252.
- Fatoni, A., Hariani, P.L., Hermansyah, H., Lesbani, A., 2018. Synthesis and characterization of chitosan linked by methylene bridge and Schiff base of 4, 4-Diaminodiphenyl ether-vanillin. *Indones. J. Chem.* 18, 92–101.
- Frenkel, C., Havkin-Frenkel, D., 2006. Vanilla-Material properties: the Physics and Chemistry of Vanillin-Research sheds light on practical ways to prevent losses of vanillin during production. *Perfum. Flavor.* 31, 28–37.
- Gallage, N.J., Møller, B.L., 2018. Vanilla: the Most Popular Flavour. *Biotechnology of Natural Products*. Springer, pp. 3–24.
- Gupta, A., Saleh, N.M., Das, R., Landis, R.F., Bigdeli, A., Motamedchaboki, K., et al., 2017a. Synergistic antimicrobial therapy using nanoparticles and antibiotics for the treatment of multidrug-resistant bacterial infection. *Nano Futures* 1, 015004.
- Gupta, D., Singh, A., Khan, A.U., 2017b. Nanoparticles as efflux pump and biofilm inhibitor to rejuvenate bactericidal effect of conventional antibiotics. *Nanoscale Res. Lett.* 12, 454.
- Hariono, M., Abdullah, N., Damodaran, K., Kamarulzaman, E.E., Mohamed, N., Hassan, S.S., et al., 2016. Potential new H1N1 neuraminidase inhibitors from ferulic acid and vanillin: molecular modelling, synthesis and in vitro assay. *Sci. Rep.* 6, 38692.
- <https://www.accessdata.fda.gov/scripts/cdrh/cfdocs/cfcfr/CFRSearch.cfm?r=182.60>. Accessed - 23/12/2018.
- Iannuzzi, C., Borriello, M., Irace, G., Cammarota, M., Di Maro, A., Sirangelo, I., 2017. Vanillin affects amyloid aggregation and non-enzymatic glycation in human insulin. *Sci. Rep.* 7, 15086.
- Kalia, N.P., Mahajan, P., Mehra, R., Nargotra, A., Sharma, J.P., Koul, S., et al., 2012. Capsaicin, a novel inhibitor of the NorA efflux pump, reduces the intracellular invasion of *Staphylococcus aureus*. *J. Antimicrob. Chemother.* 67, 2401–2408.
- Kaur, A., Sharma, P., Capalash, N., 2018. Curcumin alleviates persistence of *Acinetobacter baumannii* against colistin. *Sci. Rep.* 8, 11029.
- Khan, P., Rahman, S., Queen, A., Manzoor, S., Naz, F., Hasan, G.M., et al., 2017. Elucidation of dietary polyphenolics as potential inhibitor of microtubule affinity regulating kinase 4: in silico and in vitro studies. *Sci. Rep.* 7, 9470.
- Lambert, P., 2002. Mechanisms of antibiotic resistance in *Pseudomonas aeruginosa*. *J. R. Soc. Med.* 95, 22.
- Llanes, C., Hocquet, D., Vogne, C., Benali-Baitich, D., Neuwirth, C., Plésiat, P., 2004. Clinical strains of *Pseudomonas aeruginosa* overproducing MexAB-OprM and MexXY efflux pumps simultaneously. *Antimicrob. Agents Chemother.* 48, 1797–1802.
- Lorenzi, V., Muselli, A., Bernardini, A.F., Berti, L., Pagès, J.-M., Amaral, L., et al., 2009. Geraniol restores antibiotic activities against multidrug-resistant isolates from gram-negative species. *Antimicrob. Agents Chemother.* 53, 2209–2211.
- Martins, M., McCusker, M.P., Viveiros, M., Couto, I., Fanning, S., Pagès, J.-M., et al., 2013. A simple method for assessment of MDR bacteria for over-expressed efflux pumps. *Open Microbiol. J.* 7, 72.
- Mesaros, N., Glupczynski, Y., Avrain, L., Caceres, N.E., Tulkens, P.M., Van Bambeke, F., 2007. A combined phenotypic and genotypic method for the detection of Mex efflux pumps in *Pseudomonas aeruginosa*. *J. Antimicrob. Chemother.* 49, 378–386.
- Miladi, H., Zmantar, T., Chaabouni, Y., Fedhila, K., Bakhruf, A., Mahdouani, K., et al., 2016. Antibacterial and efflux pump inhibitors of thymol and carvacrol against food-borne pathogens. *Microb. Pathog.* 99, 95–100.
- Mishra, M., Kumar, S., Majhi, R.K., Goswami, L., Goswami, C., Mohapatra, H., 2018. Antibacterial efficacy of polysaccharide capped silver nanoparticles is not compromised by AcrAB-TolC efflux pump. *Front. Microbiol.* 9.
- Moghaddam, K.M., Iranshahi, M., Yazdi, M.C., Shahverdi, A.R., 2009. The combination effect of curcumin with different antibiotics against *Staphylococcus aureus*. *Int. J. Green Pharm.* 3.
- Negi, N., Prakash, P., Gupta, M.L., Mohapatra, T.M., 2014. Possible role of curcumin as an efflux pump inhibitor in multi drug resistant clinical isolates of *Pseudomonas aeruginosa*. *J. Clin. Diagn. Res.: J. Clin. Diagn. Res.* 8, DC04.
- Patel, J.B., 2017. Performance Standards for Antimicrobial Susceptibility Testing. Clinical and Laboratory Standards Institute.
- Piddock, L.J., 2006. Clinically relevant chromosomally encoded multidrug resistance efflux pumps in bacteria. *Clin. Microbiol. Rev.* 19, 382–402.
- Poole, K., 2007. Efflux pumps as antimicrobial resistance mechanisms. *Ann. Med.* 39, 162–176.
- Raghavan, B.S., Kondath, S., Anantanarayanan, R., Rajaram, R., 2015. Kaempferol mediated synthesis of gold nanoparticles and their cytotoxic effects on MCF-7 cancer cell line. *Process Biochem.* 50, 1966–1976.
- Savli, H., Karadenizli, A., Kolayli, F., Gundes, S., Ozbek, U., Vahaboglu, H., 2003. Expression stability of six housekeeping genes: a proposal for resistance gene quantification studies of *Pseudomonas aeruginosa* by real-time quantitative RT-PCR. *J. Med. Microbiol.* 52, 403–408.
- Schmittgen, T.D., Livak, K.J., 2008. Analyzing real-time PCR data by the comparative C T method. *Nat. Protoc.* 3, 1101.
- Simoes, M., Bennett, R.N., Rosa, E.A., 2009. Understanding antimicrobial activities of phytochemicals against multidrug resistant bacteria and biofilms. *Nat. Prod. Rep.* 26, 746–757.
- Sindhu, K., Rajaram, A., Sreeram, K., Rajaram, R., 2014. Curcumin conjugated gold nanoparticle synthesis and its biocompatibility. *RSC Adv.* 4, 1808–1818.
- Singh, D.K., Jagannathan, R., Khandelwal, P., Abraham, P.M., Poddar, P., 2013. In situ synthesis and surface functionalization of gold nanoparticles with curcumin and their antioxidant properties: an experimental and density functional theory investigation. *Nanoscale* 5, 1882–1893.
- Singh, P., Pandit, S., Mokkapat, V., Garg, A., Ravikumar, V., Mijakovic, I., 2018. Gold nanoparticles in diagnostics and therapeutics for human cancer. *Int. J. Mol. Sci.* 19, 1979.
- Siriyong, T., Srimanote, P., Chusri, S., Yingyongnarongkul, B-e, Suaisom, C., Tipmanee, V., et al., 2017. Connexin as a novel inhibitor of multidrug efflux pump systems in *Pseudomonas aeruginosa*. *BMC Complement Altern. Med.* 17, 405.
- Smith, D.J., Ramsay, K.A., Yerkovich, S.T., Reid, D.W., Wainwright, C.E., Grimwood, K., et al., 2016. Pseudomonas aeruginosa antibiotic resistance in australian cystic fibrosis centres. *Respirology* 21, 329–337.
- Stavri, M., Piddock, L.J., Gibbons, S., 2006. Bacterial efflux pump inhibitors from natural sources. *J. Antimicrob. Chemother.* 59, 1247–1260.
- Tegos, G., Stermitz, F.R., Lomovskaya, O., Lewis, K., 2002. Multidrug pump inhibitors uncover remarkable activity of plant antimicrobials. *Antimicrob. Agents Chemother.* 46, 3133–3141.
- Venter, H., Mowla, R., Ohene-Agyei, T., Ma, S., 2015. RND-type drug efflux pumps from Gram-negative bacteria: molecular mechanism and inhibition. *Front. Microbiol.* 6, 377.
- Ventola, C.L., 2015. The antibiotic resistance crisis: part 1: causes and threats. *Pharm. Therapeut.* 40, 277.
- WHO, 2017. WHO Publishes List of Bacteria for Which New Antibiotics Are Urgently Needed. WHO, Geneva, Switzerland.
- Yoneda, K., Chikumi, H., Murata, T., Gotoh, N., Yamamoto, H., Fujiwara, H., et al., 2005. Measurement of *Pseudomonas aeruginosa* multidrug efflux pumps by quantitative real-time polymerase chain reaction. *FEMS Microbiol. Lett.* 243, 125–131.
- Zhao, Y., Jiang, X., 2013. Multiple strategies to activate gold nanoparticles as antibiotics. *Nanoscale* 5, 8340–8350.
- Zhao, Y., Tian, Y., Cui, Y., Liu, W., Ma, W., Jiang, X., 2010. Small molecule-capped gold nanoparticles as potent antibacterial agents that target gram-negative bacteria. *J. Am. Chem. Soc.* 132, 12349–12356.